Chemical Engineering Journal 161 (2010) 377–383

Contents lists available at ScienceDirect

Chemical Engineering Journal

journal homepage: www.elsevier.com/locate/cej

Experimental and theoretical study of pyrazole *N*-alkylation catalyzed by basic modified molecular sieves

Inês Matos[a,b], Elena Pérez-Mayoral[a,*], Elena Soriano[c], Arnošt Zukal[d], Rosa M. Martín-Aranda[a], Antonio J. López-Peinado[a], Isabel Fonseca[b], Jiří Čejka[d,**]

[a] Departamento de Química Inorgánica y Química Técnica, Facultad de Ciencias, UNED, Paseo Senda del Rey 9, 28040 Madrid, Spain
[b] REQUIMTE, FCT-UNL, Lisboa, Portugal
[c] Laboratorio de Radicales Libres y Química Computacional (IQOG, CSIC), C/ Juan de la Cierva 3, 28006 Madrid, Spain
[d] J. Heyrovský Institute of Physical Chemistry, Academy of Sciences of the Czech Republic, v.v.i., Dolejškova 3, 182 23 Prague 8, Czech Republic

ARTICLE INFO

Article history:
Received 19 May 2009
Received in revised form
18 September 2009
Accepted 22 September 2009

Keywords:
Pyrazole alkylation
Basic mesoporous materials
Reaction mechanism
Theoretical calculations

ABSTRACT

Herein we report on the experimental and theoretical study of pyrazole alkylation catalyzed by basic mesoporous materials. (Cs)Al-SBA-15 or DEAPTS/MCM-4,1 differing in textural properties and compositions, were found to be efficient catalysts for pyrazole alkylation with different reactive alkyl bromides under thermal activation. They constitute the first examples of modified molecular sieves catalyzing this highly used transformation, showing a higher catalytic activity than other previously reported catalysts. DEAPTS/MCM-41 whose catalytic centers are tertiary amines resulting in the best catalyst for the investigated reactions. Furthermore, the catalytic pyrazole alkylation has been clarified by studying the reaction mechanism using computational approach.

1. Introduction

Heterocyclic compounds have a special place among natural products and synthetic compounds. More specifically, nitrogen heterocycles are abundant in nature existing in many natural products such as vitamins, hormones, antibiotics, and alkaloids, the last receiving particular attention due to their specific pharmacological activities [1].

Pyrazole, a five-membered nitrogen heterocycle, gives name to an alkaloid family being Withasomnine a representative agent (Fig. 1); this pyrazole-alkaloid is isolated from the roots of the Indian medicinal plants and used for the treatment of enlarged spleen, migraine, infection and dysentery [2,3]. Furthermore, the pyrazole ring is present on the skeleton of a large variety of compounds with biological activity such as the tetracycle **1** [4] or the pyrazolo[3,4-*c*]pyridazines **2** [5], among others (Fig. 1).

N-alkylation of pyrazole ring is a synthetic approach useful in the preparation of building blocks for the synthesis of important active compounds, like pharmaceuticals [6] and agrochemicals [7]. Thus, lidocaine analogues **3** [8] and alkynyl pyrazoles **4** [9] exhibiting muscarinic properties, or the selenium derivative **5** [10], as synthetic intermediate for the preparation of Withasomnine, have been synthesized using this methodology (Fig. 1).

In general, *N*-alkyl pyrazoles are prepared from the corresponding 1,3-dicarbonyl compounds by reaction with the pertinent substituted-hydrazines, or via alkylation of the heterocyclic ring using an excess of alkyl halides or dialkyl sulfates. Pyrazole alkylation often uses stoichiometric amounts of bases [11] even proceeding under phase transfer conditions (PTC) [12,13]. Clean technologies like microwave irradiation in the absence or the presence of bases have been also reported [14].

In order to minimize the residue formation and hence for environmental protection and also for avoiding hazardous starting materials, Ono et al. [15] reported the alkylation of pyrazole with alcohols over acidic zeolites in vapour phase. Concerning the alkylation of pyrazole with halides in basic medium as a wide scope methodology, different basic-supported catalysts such as CsF-Celite [16], KF-Al_2O_3 [17,18], CsF-Al_2O_3 and KOH-Al_2O_3 [18] have been reported.

In this context, our current interest is focused on the design, synthesis and characterization of basic molecular sieves able to efficiently catalyze this reaction. Thus, we here report on an efficient protocol for the *N*-alkylation of pyrazole ring catalyzed by basic mesoporous materials. We have chosen Al-SBA-15 incorporating Cs^+ ions [19] and functionalized MCM-41 materials with diethylamino propyl (DEAPTS) groups catalyzing the reaction with

* Corresponding author. Tel.: + 34 91 398 9047; fax: +34 91 398 66 97.
** Corresponding author. Fax: +420 28658 2307.
E-mail addresses: eperez@ccia.uned.es (E. Pérez-Mayoral), jiri.cejka@jh-inst.cas.cz (J. Čejka).

1385-8947/$ – see front matter © 2009 Elsevier B.V. All rights reserved.
doi:10.1016/j.cej.2009.09.040

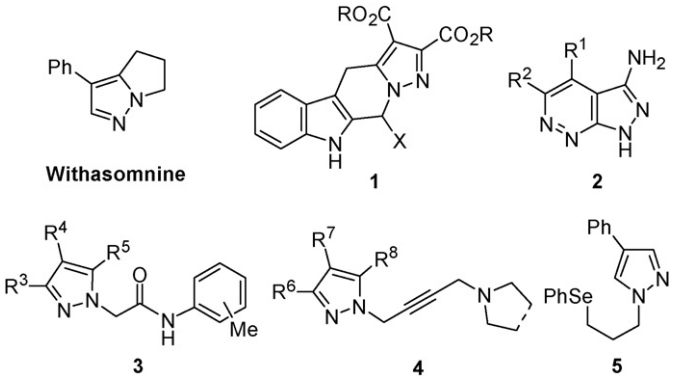

Fig. 1. Pyrazolo-derivatives with biologycal activity.

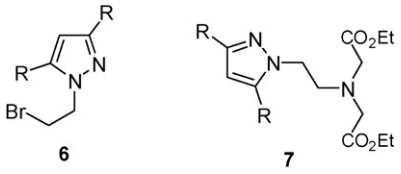

Fig. 2. Compounds **6** as key intermediates for the synthesis of **7**.

different reactive bromides under thermal activation. We have prepared the bromoethylpyrazoles **6** and the chelators **7**, whose Gd(III)-complexes of the corresponding carboxylic acids are considered as T_2 relaxation agents for Magnetic Resonance Imaging (Fig. 2) [13]. Moreover, we also report a DFT-based theoretical analysis in order to get a deeper insight into the reaction mechanism and to explain the catalytic activity of our novel mesoporous catalysts.

2. Material and methods

2.1. General

NMR spectra were recorded with a Bruker DRX-400 (400.13 MHz for ^{1}H, and 100.033 MHz for ^{13}C). ^{1}H and ^{13}C chemical shifts (δ) in $CDCl_3$ are given from internal tetramethylsilane. TLC chromatography was performed on DC-Aulofolien/Kieselgel 60 F245 (Merck) and column chromatography, though silica gel Merck 60 (230–400 mesh). The evolution of the reactions was followed by gas chromatography, Agilent 6890 GC (HP5 column, 30 m 0.32 mm), the final conversion being determined by ^{1}H NMR.

All the reagents and solvents were obtained from Aldrich.

2.2. Catalyst preparation

2.2.1. (Cs)Al-SBA-15

The (Cs)-Al-SBA-15 was prepared from Al-SBA-15 [20] following the synthetic protocol described by Pérez-Mayoral et al. [19].

2.2.2. APTS/MCM-41

Amino-grafted MCM-41 materials were synthesized according the experimental procedure reported in the literature [21] starting from MCM-41 support and the corresponding trialkoxysilylpropylamine. In more detail, 35 ml of toluene was added to 2 g of dried MCM-41, then 6.65×10^{-3} mol (molar excess) of (3-aminopropyl)trimethoxysilane (APTMS) was added and the mixture was stirred for 5 h at room temperature (296 K). Then toluene was filtered off and the modified MCM-41 was washed out three times with 20 ml of toluene and finally the modified MCM-41 was dried in vacuum at room temperature.

2.2.3. DEAPTS/MCM-41

DEAPTS/MCM-41 was prepared by the same procedure described above and using the same molar excess (6.65×10^{-3} mol) of the corresponding amino linker and 2 g of dried molecular sieve MCM-41.

2.3. Catalyst characterization

The surface area of the catalysts under study was determined by measurement of adsorption isotherms of nitrogen at 77 K applying the BET method using a static volumetric apparatus Micromeritics, ASAP 2020 (Table 1). In order to attain a sufficient accuracy in the accumulation of the adsorption data, this instrument is equipped with pressure transducers covering the 133 Pa and 133 kPa ranges. Before each sorption measurement the samples were outgassed at 313 K overnight until the residual pressure was lower than 0.7 Pa.

Thermal stability of the solids based on MCM-41 structure was investigated by TG experiments using a TA Instrument SDT Q600. Furthermore, the quantitative measurements of the basic active centers over MCM-41 materials were determined by chemical analysis whereas the Al/Si relationship and Cs loading on SBA-15 materials were measured by ICP-MS (Table 1).

2.4. N-Alkylation procedures

2.4.1. Alkylation of pyrazole

To a solution of the corresponding pyrazole (2 mmol) in the respective solvent (5 mL; acetonitrile or DMF) 20 wt% of the catalyst with regard to pyrazole was added and the mixture was stirred for 5 min. Subsequently, the corresponding alkyl bromide (10–20 mmol) was added and the reaction mixture was stirred at the given temperature for the time shown in Table 2. After cooling, the catalyst was filtered and the solvent was removed *in vacuo*.

Reaction crudes resulting of the alkylation of **8a** and **8b** with 1,2-dibromoethane (catalyst: DEAPTS) were purified by flash column chromatography on silica gel using as eluent a mixture of CH_2Cl_2/EtOH (99:1) yielding compounds **6d** and **6e** in 89% and 93%, respectively.

2.4.2. Alkylation of diethyl iminodiacetate

To a solution of diethyl iminodiacetate (2 mmol) in the corresponding solvent (5 mL; acetonitrile or DMF) 5 wt% of the catalyst

Table 1
Structural parameters of the catalysts.

Catalysts	S_{BET}[a] (m^2/g)	V_{MESO}[b] (cm^3/g)	D_{MESO}[b] (nm)	Cs[c] (%)	Al/Si[c]	C[d] (%)	N[d] (%)
(Cs)Al-SBA-15[e]	435.9	0.74	5.6	3.8	0.21	–	–
APTS/MCM-41	640.0	0.71	3.2	–	–	6.64	2.16
DEAPTS/MCM-41	587.8	0.67	3.0	–	–	11.87	1.93

[a] S_{BET}, BET surface area.
[b] V_{MESO} and D_{MESO}, mesopore volume and mesopore diameter, respectively, calculated using BJH method.
[c] Determined by ICP-MS.
[d] Measured by elemental analysis.
[e] See Ref. [19].

Table 2
Alkylation of pyrazole with different reactive alkyl bromides.

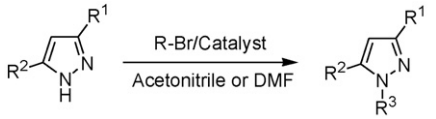

6a: R^1= R^2 = H; R^3 = -CH_2Ph,
6b: R^1= R^2 = H; R^3 = -CH_2-CH=CH_2,
6c: R^1= R^2 = H; R^3 = -CH_2CO_2Et,
6d: R^1= R^2 = H; R^3 = -CH_2CH_2Br
6e: R^1= R^2 = Me; R^3 = -CH_2CH_2Br

8a: R^1= R^2 = H
8b: R^1= R^2 = Me

Entry	R–Br	Catalyst	Solvent	Temperature (K)	Time (h)	Conversion to 6 (%)
1	$PhCH_2Br$	(Cs)Al-SBA-15	CH_3CN	rt	2	68
2		(Cs)Al-SBA-15	CH_3CN	353	30 min	96
3	CH_2=$CHCH_2Br$	(Cs)Al-SBA-15	CH_3CN	338	80 min	90
4		DEAPTMS	CH_3CN	338	1	96
5	CH_2CO_2Et	(Cs)Al-SBA-15	CH_3CN	353	3	51
6		(Cs)Al-SBA-15	DMF	373	2	93[a]
7		DEAPTMS	DMF	373	2	90
8	$BrCH_2CH_2Br$	(Cs)Al-SBA-15	DMF	373	3	84
9		DEAPTMS	DMF	373	3	93 (97)[b]
10		DEAPTMS	Free-solvent	373	3	**6d**: 76 **9**: 18

Evolution of the reactions was followed by GC analysis.
Conversions were determined by ^{1}H NMR on the crude products.
[a] Reactions were completed during 3 h.
[b] Reagent, solvent and catalyst amounts were doubled.

with regard to amine was added and the mixture was stirred for 5 min. Subsequently, the corresponding alkyl bromide (2 mmol) was added and the reaction mixture was stirred at the given temperature for the time shown in the Table 3. After cooling, the catalyst was filtered and the solvent was removed *in vacuo*.

All *crude products* are characterized by ^{1}H NMR and MS; spectroscopic data for allyl pyrazole (**6b**) [12] and benzyl pyrazole (**6a**) [16] and compounds **6d-e** and **7a-b** [13] are according to those previously reported.

2.4.3. Spectroscopic data of compounds *6c*, *10*

Pyrazole-1-carboxylic acid ethyl ester (6c): δ_H (400 MHz; $CDCl_3$) 7.49, 7.48 (2H, 2 s, H-3 and H-5), 6.25 (1H, s, H-4), 4.98 (2H, s, N–CH_2), 4.15 (2H, q *J* = 7.2, CH_2O), 1.20 (3H, t *J* = 7.2 Hz, CH_3); MS (EI): *m*/*z* (%) 154 (M^+, 25), 81 (65), 73 (100).

(Allyl-ethoxycarbonylmethyl-amino)-acetic acid ethyl ester (10): δ_H (400 MHz; $CDCl_3$) 5.93–5.84 (1H, m, CH=CH_2), 5.25–5.17 (2H, m, CH=CH_2), 4.14 (4H, q *J* 7.2 Hz, CH_2O), 3.65 (4H, s, N–CH_2–CO), 3.47 (2H, d *J* = 7.2 Hz, CH_2–CH=CH_2), 1.27 (6H, t *J* 7.2 Hz, CH_3); MS (EI): *m*/*z* (%) 229 (M^+, 16), 156 (100), 116 (88).

2.5. Theoretical calculations

Cluster calculations have been performed with Gaussian03 [22]. Geometry optimizations have been performed with the density functional theory (DFT) using the Becke's three-parameter hybrid method with the Lee-Yang-Parr correlation functional (B3LYP) [23] and the 6-31G* basis set for all atoms.

The vibrational frequencies were computed by using analytical second derivatives to check that the stationary points found exhibit the proper number of imaginary frequencies: none for a minimum and one for a transition state (first-order saddle point) that indeed corresponds to the expected motion of atoms along the reaction coordinate. Zero point energy (ZPE) corrections have been calculated for all optimized structures. The intrinsic reaction-coordinate (IRC) [24] pathways from the transition structure have been followed by using a second-order integration method [25], to verify the proper connections with reactants and products.

3. Results and discussion

3.1. Characterization of the catalysts

Table 1 shows the textural parameters of the catalysts under study. Both of them exhibit different structural parameters, enhancing the pore size in a range of 3.2–5.6 nm. There are no significant differences regarding the surface area of the MCM-41 materials but it is higher in comparison with that for the caesium catalyst. In all cases mesoporous volumes approximately are about 0.7 cm^3/g. Al/Si relationship and Cs loading on the SBA-15 were 0.21% and 3.8%, respectively, both of them determined by ICP-MS (Table 1). The %C supported onto MCM-41 materials were 11.87 and 6.64 whereas %N were 1.93%, and 2.16% both for DEAPTS/MCM-41 and APTS/MCM-41, respectively, measured by elemental analysis as shown in Table 1. Similar nitrogen percentage suggests the same concentration of amine groups for the MCM-41 materials. Finally,

Table 3
Alkylation of diethyl iminodiacetate.

Entry	R–Br	Catalyst	Solvent	Temperature (°C)	Time (h)	Conversion (%)
1	$BrCH_2CH$=CH_2	DEAPTMS	CH_3CN	rt	0.5	96
2		(Cs)Al-SBA-15	CH_3CN	rt	3	96
3	**6d**	DEAPTMS	DMF	373	4.5	79[a]
4	**6e**	DEAPTMS	DMF	373	4	81[a]

Evolution of the reactions was followed by GC analysis.
Conversions were determined by ^{1}H NMR on the crude products.
[a] 0.5 mmol of the corresponding bromide and amine were used in 2 ml of DMF as solvent. Catalyst amount: 20 wt% with regard to the amine.

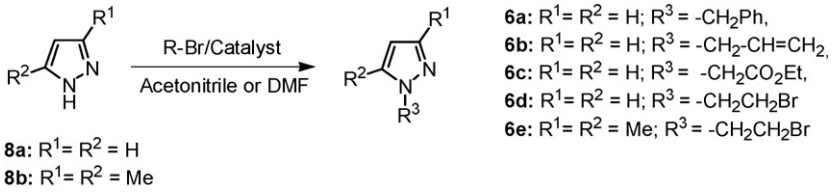

Scheme 1. Alkylation of pyrazole ring with different reactive alkyl bromides.

the thermal stability of both catalysts was studied by thermogravimetric experiments, both samples being stables up to 200 °C.

3.2. Alkylation reaction pyrazoles

As far as we know, there are only a few examples of basic catalysts, modified Celite or Al_2O_3, for the preparation of the *N*-alkyl pyrazoles as commented above [16,17,18]. Note that these catalysts have been exclusively used in the benzylation of pyrazole, benzyl bromide being one of the most reactive bromides.

Based on that, we report on the pyrazole alkylation catalyzed by basic molecular sieves, (Cs)Al-SBA-15 and DEAPTMS/MCM-41 being the catalysts of choice. The silica surface has been modified by caesium cations or aminopropyl groups both of them controlling to the basicity of those catalysts.

Thus, *N*-alkylation of pyrazole **8a** with alkyl bromides was carried out using acetonitrile or DMF as solvents for this reaction, in a temperature range of 298–373 K, in the presence of the catalysts (20 wt% with regard to the pyrazole), affording the corresponding *N*-substituted pyrazole **6** with high yields (Table 2 and Scheme 1). All reactions have been performed in the presence of an excess of the corresponding alkyl bromide since these experimental conditions were required in order to selectively synthesize the compounds **6d-e**.

In order to select the best experimental conditions, we carried out the benzylation of pyrazole **8a** catalyzed by (Cs)Al-SBA-15 in acetonitrile at room temperature and by refluxing on that, respectively (Table 2; entries 1 and 2). When the reaction was performed at room temperature during two hours, *N*-benzyl pyrazole (**6a**) was obtained with 68% of conversion while the reaction at 353 K led to compound **6a** in almost quantitative yield in only 30 min (Table 2, entry 2). These data revealed that (Cs)Al-SBA-15 is an efficient catalyst for this reaction; benzylation of pyrazole **8a** took place with high conversions using smaller amount of the catalyst than those reported [17], (only 20 wt% with regard to pyrazole, 27.2 mg of our catalyst), thus, avoiding the diffusion problems that the presence of the larger solid amounts implies.

Following our ongoing investigations, we studied the alkylation of the pyrazole ring with other alkyl bromides. The reaction with allyl bromide in acetonitrile, at 338 K, led to the *N*-allyl pyrazole (**6b**) with 90% and 96% of yield, during 80 and 60 min, when using (Cs)Al-SBA-15 and DEAPTMS/MCM-41, respectively (Table 2; entries 3 and 4).

On the other hand, we carried out the alkylation using ethyl bromoacetate as a less reactive alkylating agent; the alkylation was achieved in the presence of (Cs)Al-SBA-15 in acetonitrile, at 353 K for 3 h, affording the compound **6c** with moderate conversion (51%) (Table 2; entry 5). In order to reduce the reaction time and to improve the conversion, the reaction was performed at higher temperature (373 K). During 2 h, in DMF as solvent, the alkylated *N*-pyrazole **6c** in 93% yield was obtained. This reaction also proceeded using the same reaction conditions in the presence of DEAPTMS/MCM-41 yielding similar conversions (Table 2; entries 6 and 7).

Finally, the reaction between pyrazole **8a** and 1,2-dibromo ethane was carried out at 373 K employing DMF as solvent. In this case, the bromoethyl pyrazole **6d** was selectively obtained with 84% and 93% of yield catalyzed by (Cs)Al-SBA-15 and DEAPTMS/MCM-41, respectively (Table 2; entries 8 and 9). Note that whereas the alkylation in the presence of DMF selectively led to the product **6d**, using free-solvent conditions and excess of 1,2-dibromo ethane, a mixture of the compounds **6d** (70%) and **9** (26%) was isolated, compound **6d** being the major product (Table 2; entry 10, Scheme 2). It is important to stress that when the alkylation is made in DMF, at 373 K, dimethyl amonium bromide was isolated as a decomposition product of the solvent in the presence of HBr; this by-product was easily removed by precipitation with acetone and identified by ^{1}H and ^{13}C NMR. In order to overcoming this inconvenience, we tried the reaction in toluene but, unfortunately, only traces of compound **6d** were detected.

In conclusion, the alkylation of pyrazole **8a** catalyzed by (Cs)Al-SBA-15 and DEAPTS/MCM-41 (20 wt% regarding to pyrazole) in the presence of any solvent, acetonitrile or DMF, provided selectively the corresponding *N*-alkylpyrazole with high yields (84–96%). Our results indicate that (Cs)Al-SBA-15 and DEAPTS/MCM-41 efficiently catalyze this transformation showing higher catalytic activity than other basic catalysts reported in the literature and cited here; DEAPTS/MCM-41 was slightly more efficient catalyst than the caesium solid (Table 2; entries 3, 4, 8 and 9). Such case is the alkylation with allyl bromide; the reaction took place in acetonitrile at 338 K giving *N*-allyl pyrazole (**6c**) with good yield (96%) in only 1 h catalyzed by DEAPTS/MCM-41, whereas employing the caesium catalyst was nearly completed (90%) for 80 min at the same reaction temperature.

N-alkylation of pyrazole **8a** was also catalyzed by APTMS pattern affording the corresponding pyrazoles with similar conversions. Obviously, the amine groups of the catalyst were alkylated, and hence transformed in a mesoporous solid with similar characteristics than DEAPTS/MCM-41; this feature was confirmed by FTIR. Comparison of IR spectra of APTS/MCM-41 and that post-modified in the reaction of **8a** with ethyl bromoacetate showed the presence of the signal at 1760 cm^{-1} assigned to $\nu_{C=O}$ corresponding to the ethyl acetate motif as consequence of the amine alkylation. The catalyst maintains the hexagonal structure as indicated in the XRD experiments by the presence of the characteristic diffraction lines at low angles.

Fig. 3 depicts the progress of the alkylation of pyrazole with ethyl bromoacetate, in DMF at 373 K, catalyzed by *in situ* modified APTS and DEAPTS/MCM-41. In both cases, the final conversion to compound **6d** is nearly 100% after 3 h of the reaction time. For the catalyst bearing primary amine groups a slower reaction rate was observed, probably because of its modification by alkylation with the alkyl bromide in the reaction medium.

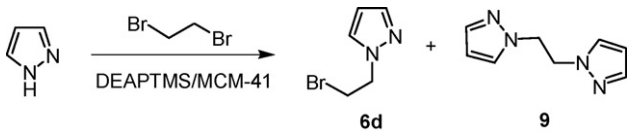

Scheme 2. Alkylation of pyrazole with 1,2-dibromoethane.

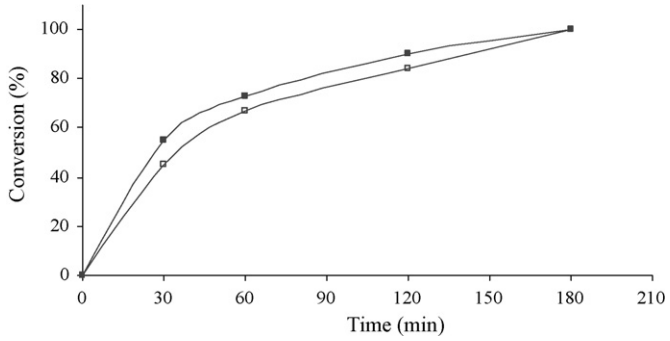

Fig. 3. Alkylation of pyrazole with ethyl bromoacetate, in DMF at 373 K, catalyzed by (■) ATMS and (□) DEAPTMS/MCM-41.

Furthermore, we investigated the optimal amount of the catalyst to be used. Thus, while the reaction catalyzed by the caesium or APTS/MCM-41 required 27.2 mg of the solid, corresponding to 20 wt% with regard to the pyrazole, in the case of DEAPTS/MCM-41 the required minimal amount was about 10 wt%. This outcome confirms the highest efficacy for DEAPTS/MCM-41.

Subsequently, we achieved the alkylation of pyrazole **8b**, using the same experimental conditions as those for the alkylation of compound **8a**, yielding the pyrazole **6e** with 97% and 91% of conversion, during 2 and 3 h, when catalyzed by DEAPTS and (Cs)Al-SBA-15, respectively (Scheme 1).

In order to prepare the compounds **7**, the catalysts under study were also employed for the alkylation of diethyl iminodiacetate by using the same experimental protocol. We firstly test our catalysts for the reaction of diethyl iminodiacetate with allyl bromide in acetonitrile at room temperature. Under these conditions the corresponding diethyl *N*-(allyl)iminodiacetate (**10**) was obtained with 96% of yield, during 30 min and 3 h, catalyzed by DEAPTS/MCM-41 and (Cs)Al-SBA-15, respectively (Table 3; entries 1 and 2). In this case, the catalyst amount used for alkylation was 5 wt% (regarding to amine), notably lower than those for the pyrazole alkylation. The synthesis of compounds **7** was then studied with bromoethyl pyrazoles **6d-e**, previously prepared by using the synthetic methodology here reported and purified by flash column chromatography, and diethyl iminodiacetate at room temperature and 353 K, in acetonitrile as solvent, with the most effective catalyst, DEAPTS/MCM-41. Under these conditions the desired compounds **7** were not detected, compounds **6d-e** being a less reactive species as expected. Therefore, the reaction was carried out in DMF at 373 K observing the formation of compounds **7a-b** with a yield around 80% for 4 and 4 h 30 min, respectively (Scheme 3 and Table 3; entries 3 and 4).

3.3. Theoretical calculations

To understand in more detail the catalytic behaviour of our best catalyst, DEAPTS/MCM-41, from its local structure, a 4T cluster including four Si tetrahedral atoms has been chosen as a model of the catalytic active center (Fig. 4). In this model, the dangling bonds were terminated with OH groups to satisfy the valencies

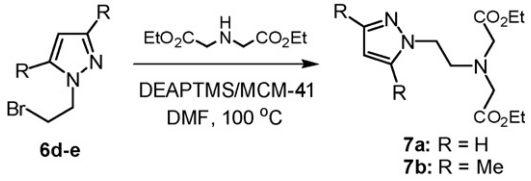

Scheme 3. Preparation of chelating ligand **7**.

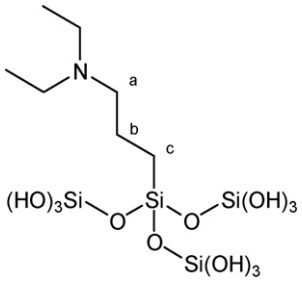

Fig. 4. 4T cluster used as a model for the theoretical study of the catalytic activity of DEAPTMS/MCM-41.

[26], i.e., the cluster model was terminated with –Si(OH)$_3$. In order to reduce the computational cost, we have compared these results with those obtained from an alternative 4T cluster where the dangling bonds are terminated with H atoms [27], i.e., the cluster model was terminated with –SiH$_3$ [28].

Recently, the cluster approach has been used in many theoretical studies to describe local phenomena of the zeolite-catalyzed reactions like the interaction of organic reactants with active sites over this catalyst, bond breaking/formation processes, etc. [29]. This approach provides a facile, computationally feasible and efficient tool to simulate the catalytic active sites on the catalyst [30], although one must bear in mind that a cluster is only a simplified model that ignores long-range effects imposed by the mesoporous catalysts [31]. Among them, in consideration of the dominant interactions occurring between the reactants and the active sites as well as their neighbour atoms, the 4T cluster [32], a small cluster model, has been widely used to investigate the reaction on the active sites. In fact, a theoretical study has indicated that the reaction trends obtained with the 4T clusters are consistent with those calculated with the larger 28T clusters [33]. Therefore, here the 4T cluster model (Fig. 4) was used to explore the catalytic properties of our solids.

Taking into account the alkylation of pyrazole with ethyl bromide as the model of the choice, we have found that pyrazole is adsorbed on the basic site of the pendant amine by means of an H-bond to form an adsorption complex $\mathbf{R_{MCM\text{-}41}}$ (Fig. 5). The acid proton of the azole is at a distance of 1.907 Å of the amine nitrogen atom. From this complex, we located the transition structure **TS** whose structural parameters suggest an advanced transition state: the distance between the attacking azole N with the plannarized carbon of the alkyl moiety is 1.986 Å, whereas the length of the partially broken C–Br bond is 2.610 Å. Although an incipient H abstraction is observed, the acidic proton still remains close to the azole (N(azole)–H distance = 1.062 Å), the amine N being at a distance of 1.811 Å. These data point out to a concerted but highly asynchronous process. In fact, IRC calculations revealed that **TS** evolves to the products (**P** complex): the alkylated azole and the HBr (1.999 Å) adsorbed on the basic site (distance N(amine)–H = 1.093 Å).

The energy profile of this reaction is depicted in Fig. 5. The activation energy required to attain the transition state is 31.0 kcal mol^{-1}, and the alkylation is an exothermic process (by −9.5 kcal mol^{-1}) (Table 4).

Finally, it is remarkable the catalytic activity of both 4T clusters, since the uncatalyzed process between the azole and the alkyl halide proceeds with an activation barrier as high as 666.0 kcal mol^{-1} being a nearly thermoneutral process (−0.8 kcal mol^{-1}). The alkylic chain is always moving but the most extended conformation is adopted during the reaction coordenate. As expected, the torsional angles are nearly constant along the reaction, thus confirming that the mesoporous material only acts as a support (Fig. 4 and Table 5).

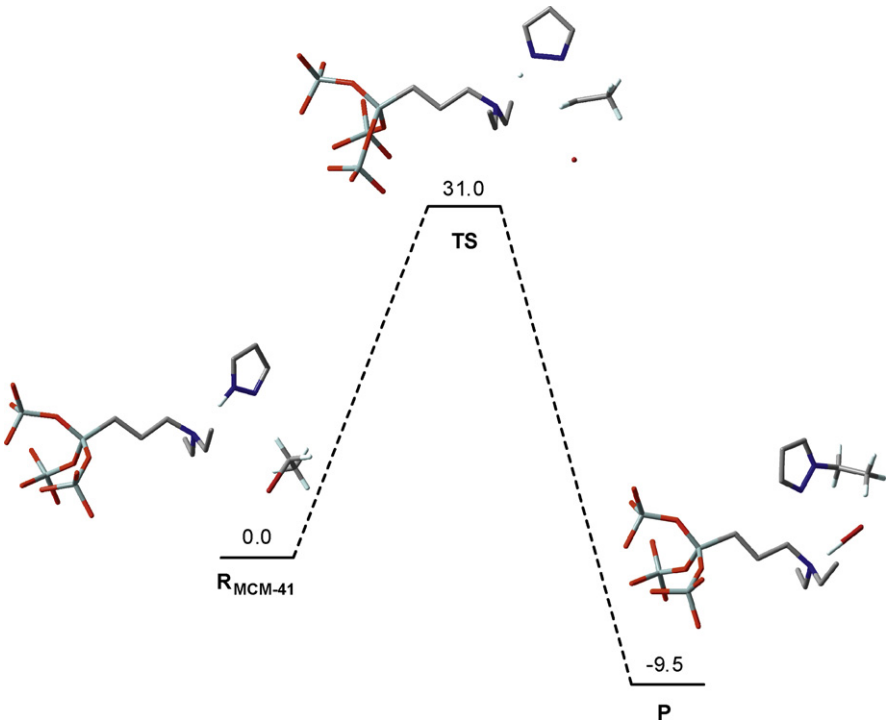

Fig. 5. Reaction free energy profile for the alkylation catalyzed by the aminopropyl group (MCM-41) (in kcal mol^{-1}). Most of the H's have been omitted for the sake of clarity.

Table 4
Enthalpy and free energy differences relative to $\mathbf{R_{MCM-41}}$ for both 4T clusters.

Cluster		ΔH (kcal mol^{-1})	ΔG (kcal mol^{-1})
4T (OH)	$\mathbf{R_{MCM-41}}$	0.0	0.0
	TS	27.7	31.0
	P	−12. 2	−9.5
4T (H)	$\mathbf{R_{MCM-41}}$	0.0	0.0
	TS	31.3	32.5
	P	−13.6	−10.8

Table 5
Variation of the torsional angles (in °) along the reaction.

	$\mathbf{R_{MCM-41}}$	TS	*P*
N–Ca–Cb–Cc	179.7	179.6	178.4
Ca–Cb–Cc–Si	179.9	178.2	178.8
Cb–Cc–Si–O	179.8	178.5	178.6

4. Conclusions

Mesoporous materials such as (Cs)Al-SBA-15 or DEAPTS/MCM-41 were investigated as efficient basic catalysts for the alkylation of pyrazole and diethyl iminodiacetate with different reactive alkyl bromides under thermal activation. In particular, DEAPTS/MCM-41 resulted in the best catalyst for this transformation. Our experimental and theoretical results demonstrated that the alkylation of pyrazole could be performed using catalytic conditions employing the smallest amounts of the solid than those reported. It avoids the necessity of using stoichiometric amounts of bases and tedious work-up procedures and therefore reducing the waste generation.

Furthermore, as far as it concerns, catalysts reported here are the first examples of modified molecular sieves catalyzing this reaction, exhibiting higher catalytic activity than other previously described.

Catalytic properties of the best catalyst, DEAPTS/MCM-41, in the pyrazole alkylation have been rationalized by using theoretical calculations. The reaction mechanism has been found to proceed in a single step promoted by the basic sites of the modified MCM-41 support, the activation barrier being notably reduced regarding the uncatalyzed process.

Methodology here communicated finds its application to the preparation of compounds **6d-e** as key intermediates for the preparation of ligands **7** and other [34,35] whose corresponding acids exhibited interesting chelating properties.

Acknowledgements

This work has been supported in part by: Spanish Ministerio de Educación y Ciencia (projects MAT2007-66439-C02-01 and CTQ2009-10478) and the Academy of Sciences of the Czech Republic (project 1QS400400560). Inês Matos thanks Fundação para Ciência e Tecnologia for grant SFRH/BPD/34659/2007.

Appendix A. Supplementary data

Supplementary data associated with this article can be found, in the online version, at doi:10.1016/j.cej.2009.09.040.

References

[1] P.M. Dewick, Medicinal Natural Products, 2nd ed., John Wiley & Sons, Ltd., Chichester, UK, 2002.
[2] H.B. Schröter, D. Neumann, A.R. Katritzky, F.J. Swinbourne, Tetrahedron 22 (1966) 2895–2897.
[3] S.A. Adesanya, R. Nita, C. Fontaine, M. Païs, Phytochemistry 35 (1994) 1053–1055.
[4] K.A. Abu-Safieh, M.M. El-Abadelah, S.S. Sabri, W. Voelter, C.M. Mössmer, M. Stroebele, Z. Naturforsch 57b (2002) 1327–1332.
[5] M.F. Braña, M. Cacho, M.L. García, E.P. Mayoral, B. López, B. de Pascual-Teresa, A. Ramos, N. Acero, F. Llinares, D. Muñoz-Mingarro, O. Lozach, L. Meijer, J. Med. Chem. 48 (2005) 6843–6854.
[6] P.J. Edwards, H.L. Jones, E.C. Mowbray, A.P. Stupple, I, Tran, Int. Appl. Pat. 2004, WO 2004/031156.
[7] K. Nebel, H.-G. Brunner, G. Pissiotas, Int. Appl. Pat. 1996, WO 96/01254.
[8] M. Iovu, C. Zalaru, F. Dumitrascu, C. Draghici, E. Cristea, Il Farmaco 55 (2000) 362–368.
[9] M.I. Rodríguez-Franco, I. Donrronsoro, A. Badía, J.E. Baños, Arch. Pharm. Pharm. Med. Chem. 7 (2002) 339–346.

[10] S.M. Allin, W.R.S. Barton, W.R. Bowman, T. McInally, Tetrahedron Lett. 43 (2002) 4191–4193.
[11] T.L. Gilchrist, Heterocyclic Chemistry, 2nd ed., Longman, London, 1992.
[12] (a) E. Diez-Barra, A. De La Hoz, A. Sánchez-Migallón, Tejeda J., Syn. Commun. 20 (1990) 2849–2853;
(b) E. Díez-Barra, A. de la Hoz, A. Loupy, A. Sánchez-Migallón, Heterocycles 38 (1994) 1367–1374.
[13] P. López, C.G. Seipelt, P. Merkling, L. Sturz, J. Álvarez, A. Dölle, M.D. Zeidler, S. Cerdán, P. Ballesteros, Bioorg. Med. Chem. 7 (1999) 517–527.
[14] I. Almena, E. Díez-Barra, A. de la Hoz, J. Ruíz, A. Sánchez-Migallón, J. Heterocycl. Chem. 35 (1998) 1263–1268.
[15] Y. Ono, Y. Izawa, Z.-H. Fu, Catal. Lett. 47 (1997) 251–253.
[16] S. Hayat, Atta-ur-Rahman, M.I. Choudhary, K.M. Khan, W. Schumann, E. Bayer, Tetrahedron 57 (2001) 9951–9957.
[17] F.M. Moghaddan, S.M. DokhTaimoory, H. Ismaili, G.R. Bardajee, Syn. Commun. 36 (2006) 3599–3607.
[18] M.W. Branco, R.Z. Cao, L.Z. Liu, G. Ege, J. Chem. Res. (S) (1999) 274–275.
[19] E. Pérez-Mayoral, R.M. Martín-Aranda, A.J. López-Peinado, P. Ballesteros, A. Zukal, J. Čejka, Top. Catal. 52 (2009) 148–152.
[20] (a) D. Zhao, Q. Huo, J. Feng, B.F. Chmelka, G.D. Stucky, J. Am. Chem. Soc. 120 (1998) 6024–6036;
(b) A. Zukal, H. Šiklová, J. Čejka, Langmuir 24 (2008) 9837–9842.
[21] H. Balcar, J. Čejka, J. Sedláček, J. Svoboda, J. Zednık, Z. Bastl, V. Bosáček, J. Vohlıdal, J. Mol. Catal. A: Chem. 203 (2003) 287–298.
[22] Gaussian 03; Gaussian, Inc.: Wallingford, CT (2004).
[23] (a) A.D. Becke, J. Chem. Phys. 98 (1993) 5648–5652;
(b) W. Lee, R.G. Yang, R. Parr, Phys. Rev. B 37 (1998) 785–789.
[24] K. Fukui, Acc. Chem. Res. 14 (1981) 363–368.
[25] C. González, H.B. Schlegel, J. Phys. Chem. 94 (1990), pp. 5523–5527.
[26] (a) L.S. Sremaniak, J.L. Whitten, M.J. Truitt, J.L. White, J. Phys. Chem. B 110 (2006) 20762–20764;
(b) M. Castellá-Ventura, Y. Akacem, E. Kassab, J. Phys. Chem. C 112 (2008) 19045–19054;
(c) I.I. Zakharov, Z.R. Ismagilov, S.Ph. Ruzankin, V.F. Anufrienko, S.A. Yashnik, O.I. Zakharova, J. Phys. Chem. C 111 (2007) 3080–3089;
(d) K. Pierloot, A. Delabie, M.H. Groothaert, R.A. Schoonheydt, Phys. Chem. Chem. Phys. 3 (2001) 2174–2183.
[27] (a) M. Boronat, P. Viruela, A. Corma, J. Phys. Chem. A 102 (1998) 9863–9868;
(b) S.R. Blaszkowski, R.A. van Santen, J. Phys. Chem. B 101 (1997) 2292–2305;
(c) Y. Jiang, M. Hunger, W. Wang, J. Am. Chem. Soc. 128 (2006) 11679–11692;
(d) H. David, J. Wells, A.M. Joshi, D.W. Nicholas, K.T. Thomson, J. Phys. Chem. B 110 (2006) 14627–14639;
(e) M. Boronat, P.M. Viruela, A. Corma, J. Am. Chem. Soc. 126 (2004) 3300–3309;
(f) I. Milas, A.M. Silva, M.A. Chaer Nascimento, Appl. Catal. A: General 336 (2008) 17–22.
[28] B. Arstad, J.B. Nicholas, J.F. Haw, J. Am. Chem. Soc. 126 (2004) 2991–3001.
[29] (a) M. Boronat, M. Claudio, Z. Wilson, P. Viruela, A. Corma, J. Phys. Chem. B 105 (2001) 11169–11177;
(b) J. Sauer, M. Sierka, F. Haase, in: D.G. Truhlar, K. Morokuma (Eds.), Transition State Modeling for Catalysis; ACS Symp. Ser. 721, American Chemical Society, Washington, DC, 1999, p. 359;
(c) P.M. Esteves, A.C. Nascimento, J.A. Mota, J. Phys. Chem. B 103 (1999) 10417–10420;
(d) G.J. Kramer, R.A. van Santen, J. Am. Chem. Soc. 117 (1995) 1766–1776;
(e) M.J. Rice, A.K. Chakraborty, A.T. Bell, J. Phys. Chem. B 102 (1998) 7498–7504.
[30] (a) G.J. Kramer, A.J.M. de Man, R.A. van Santen, J. Am. Chem. Soc. 113 (1991) 6435–6441;
(b) M.V. Frash, R.A. van Santen, Top. Catal. 9 (1999) 191–205;
(c) R.A. Van Santen, G.J. Kramer, Chem. Rev. 3 (1995) 637–660.
[31] (a) J. Sauer, in: G. Pacchioni, P.S. Bagus, F. Parmigiani (Eds.), Cluster Models for Surface and Bulk Phenomena, Plenum Press, New York, 1992, p. 533;
(b) R.A. Van Santen, J. Mol. Catal. A 115 (1997) 405–419;
(c) R.A. Van Santen, Catal. Today 30 (1997) 377–389;
(d) P. Sherwood, A.H. de Vries, S.J. Collins, S.P. Greatbanks, N.A. Burton, M.A. Vincent, I.H. Hillier, Faraday Discuss 106 (1997) 79–92.
[32] (a) J. Yuan, X. Liao, H. Wang, G. Yang, M. Tang, J. Phys. Chem. B 113 (2009) 1418–1422;
(b) B. Arstad, S. Kolboe, O. Swang, J. Phys. Chem. B 106 (2002) 12722–12726;
(c) S. Svelle, S. Kolboe, O. Swang, J. Phys. Chem. B 108 (2004) 2953–2962;
(d) A.M. Vos, R.A. Schoonheydt, F.D. Proft, P. Geerlings, J. Phys. Chem. B 107 (2003) 2001–2008.
[33] B. Chan, L. Radom, J. Am. Chem. Soc. 128 (2006) 5322–5323.
[34] E.P. Mayoral, M. García-Amo, P. López, E. Soriano, S. Cerdán, P. Ballesteros, Bioorg. Med. Chem. 11 (2003) 5555–5567.
[35] P. Ballesteros, E. Pérez-Mayoral, Int. Appl. Pat. 2005, WO/2006/051143; Int. Appl. Pat. 2005, WO/2006/051142.